Percolation of straight slots on a square grid

Alexander S. Balankin [1], M. A. Martinez-Cruz [1], F. J. Dorantes Benavidez [1], and Baltasar Mena [2]
[1]*ESIME-Zacatenco, Instituto Politécnico Nacional, Ciudad de México 07738, Mexico*
[2]*Instituto de Ingeniería, Universidad Nacional Autónoma de México, Ciudad de Mexico 04510, México*

(Received 19 February 2024; accepted 5 April 2024; published 29 April 2024)

This work is devoted to the emergence of a connected network of slots (cracks) on a square grid. Accordingly, extensive Monte Carlo simulations and finite-size scaling analysis have been conducted to study the site percolation of straight slots with length l measured in the number of elementary cells of the grid with the edge size L. A special focus was made on the dependence of the percolation threshold $p_C(l, L)$ on the slot length l varying in the range $1 \leqslant l \leqslant L-2$ for the square grids with edge size in the range $50 \leqslant L \leqslant 1000$. In this way, we found that $p_C(l, L)$ strongly decreases with increase of l, whereas the variations of $p_C(l = \text{const}, L)$ with the variation of ratio l/L are very small. Consequently, we acquire the functional dependencies of the critical filling factor and percolation strength on the slot length. Furthermore, we established that the slot percolation model interpolates between the site percolation on square lattice ($l = 1$) and the continuous percolation of widthless sticks ($l \to \infty$) aligned in two orthogonal directions. In this regard, we note that the critical number of widthless sticks per unit area is larger than in the case of randomly oriented sticks. Our estimates for the critical exponents indicate that the slot percolation belongs to the same universality class as standard Bernoulli percolation.

DOI: 10.1103/PhysRevE.109.044152

I. INTRODUCTION

Percolation models allow us to study a vast variety of phenomena in systems of different nature, ranging from a gelation in polymers and transport processes in disordered media [1,2] to biological and social contagions [3,4]. The notion of percolation refers to the emergence of a connected cluster that spans an entire system [5]. In the classic model of lattice site percolation a single site is randomly chosen at each step. Once the occupation probability p achieves a critical value p_C there appears a percolation cluster [6]. Generalizations of this model include models in which a group of neighboring sites is occupied at each iteration step [7]. A chosen group can be of any shape with fixed or variable sizes. Examples include linear, curved, cyclic, and branched k-mers [8–12]. In the literature, most attention was focused on the models in which an overlapping between percolating items is forbidden [13–15]. Only a few works were devoted to models allowing for the overlapping of percolating items on periodic lattices [16,17]. In both cases the percolation features depend on the alignment of percolating items, as well as on their geometry and sizes.

The extensions of lattice percolation include the models of continuum percolation of impermeable objects [18–20] and overlapping voids [21–24]. In the former case the role of the control parameter plays the notion of excluded volume. In the case of overlapping voids the percolation is governed by the filling factor η which is defined as the total volume (area) of all voids in a system normalized by the system volume (area). Since locations of slots are random and mutually independent, the probability that an elementary cell of the grid belongs to a void is equal to

$$p = 1 - (1 - \upsilon/V)^N = 1 - (1 - \eta/N)^N,$$

where V is the system volume, υ is the volume of elementary void (cell), N is the number of voids in the grid, and $\eta = \upsilon N/V$ is the filling factor. Taking into account that for larger N we have $(1-\eta/N)^N \approx 1-\eta \approx \exp(-\eta)$, the total porosity can be related to the filling factor as

$$p = 1 - \exp(-\eta), \tag{1}$$

when $N \to \infty$. Notice that in the literature the filling factor η is sometimes also called the reduced number density (see, for instance, Ref. [22]).

Different models of percolation are widely used to study transport phenomena in porous and/of fractured media [25,26]. In this context, a percolation cluster formed from individual voids (cracks) can be viewed as a fracture network [27,28]. The geometry of cracks and their sizes can be either fixed constants or distributed according to a statistical law [29]. In the case of rectangular individual voids the critical filling factor is adjusted by the void aspect ratio and angular distribution of void orientation [30]. In the limiting case of widthless cracks (sticks) which can intersect with each other the percolation is controlled by the stick alignment and length [31–33].

Although the effect of anisotropy in the stick orientation distribution was addresses in the literature [33], the most efforts were focused on the case of randomly oriented sticks [32]. At the same time, it was recognized that the fracture networks frequently display a strong anisotropy with two (or more) preferred directions [34,35]. In this background it was proposed that the fracture network formation can be mapped onto a model of straight slot percolation on a square grid with edge size L [36]. Each straight slot of length l consists from l open neighboring cells of unit size on the grid, while L is measured as the numbers of cells in the slot. A fluid can move between the neighboring open cells, and so it can flow

 ©2024 American Physical Society

between two regions if there is an open path between them through the fracture network. In Ref. [36] it was recognized that the threshold porosity of medium with fracture network decreases with the increases of slot length. However, the slot percolation model was not yet studied quantitatively.

The present work is devoted to study the percolation of straight slots on a square grid. A key question in percolation theory regards the percolation threshold, above which appears a percolation cluster. Another fundamental issue in the percolation theory concerns the universality class of the percolation phase transition. Accordingly, our study was focused on the effects of slot length on the percolation threshold and the scaling properties of percolation cluster formed by the straight slots on a square grid. For this purpose we have performed extensive Monte Carlo simulations and finite-size scaling analysis. Consequently, we suggest the functional approximations for the critical filling factor and the percolation strength. This allows us to establish that the slot percolation model interpolates between the site percolation on square lattice and the continuous percolation of widthless sticks aligned in two orthogonal directions. Finally, we found the critical exponents and recognize that the slot percolation belongs to the same universality class as standard Bernoulli percolation. The rest of paper is organized as follow. Section II is devoted to the details of numerical simulations. The results of Monte Carlo simulations are presented and discussed in Sec. III. The main findings and conclusions are summarized in Sec. IV.

II. DETAILS OF NUMERICAL SIMULATIONS

In this work we studied the percolation of straight slots on square grids with periodic boundary conditions. Each slot consists of l neighboring empty cells of unit size aligned along either vertical or horizontal direction in the grid of size $L \times L$. Notice that the studied system is essentially discrete and has three characteristic length: L, l, and the cell size w. Without the loss of generality the cell size can be assumed to be equal to $w = 1$. Numerical simulations start from a grid in which all cells are closed. At each iteration step a single cell is chosen by random sampling with replacement. The corresponding slot is formed by the chosen cell together with $(l-1)$ neighboring cells aligned either in the vertical direction (from bottom to top) for odd iteration steps, or in the horizontal direction (from left to right) for even iteration steps. The slots can overlap and cross each other, as it is illustrated by Fig. 1. Monte Carlo simulations were performed on square grids with side lengths $L = 50,\ 100,\ 125,\ 150,\ 200,\ 300,\ 400$, and 500. The slot length was varied in the range $1 \leqslant l \leqslant L-2$. Additionally, we performed the simulations of slots with $l = 30$ on the square grid with $L = 1000$. At least 10^3 independent runs were performed for each pair of (l, L).

The percolation cluster emerges when the concentration of open cells p exceeds a critical value $p_C(l)$. Different definitions of percolation cluster for the site percolation with periodic boundary conditions were discussed in Refs. [31–33]. Despite the periodic boundary conditions, in this work the percolation cluster is defined as the cluster that connects opposite sides of the square grid in either horizontal or vertical directions, or both. For illustration, Fig. 2 shows the percolation clusters formed by straight slots of different length on the square grid with edge size $L = 50$.

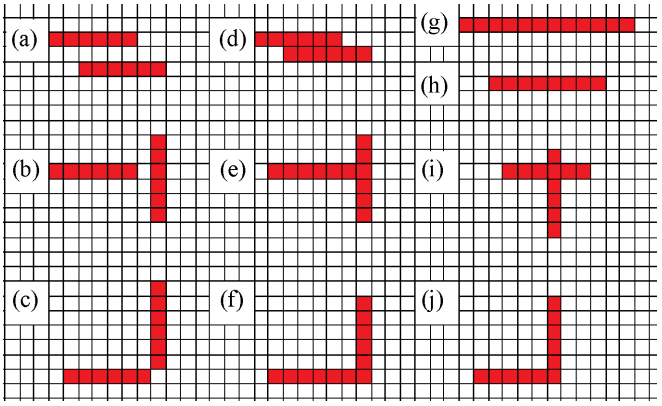

FIG. 1. Possible arrangements of two slots of length $l = 6$ on the square grid: (a), (b) two nonoverlapping slots, (c) two slots touching at corners are considered unconnected; (d)–(f) two slots sharing edges are considered connected; (g), (h) two overlapping slots are considered connected; (i), (j) two crossing slots are considered connected.

In our simulations, one slot was added at each iteration step until the percolation cluster connected the grid sides in both directions. This allows us to define four spanning probabilities. Namely, the probabilities that the percolation cluster spans the grid in the horizontal direction $R^{\mathrm{h}}_{L,l}(p)$, in the vertical direction $R^{\mathrm{v}}_{L,l}(p)$, in either horizontal or vertical direction $R^{\mathrm{or}}_{L,l}(p)$, or in both directions $R^{\mathrm{both}}_{L,l}(p)$. In this regard we note that for the studied model of slot percolation on square grids the spanning probabilities obey the following relations:

$$R^{\mathrm{both}}_{L,l} \leqslant R^{\mathrm{h}}_{L,l} = R^{\mathrm{v}}_{L,l} = R^{\mathrm{l}}_{L,l} = \left(R^{\mathrm{or}}_{L,l} + R^{\mathrm{both}}_{L,l}\right)/2 \leqslant R^{\mathrm{or}}_{L,l}, \quad (2)$$

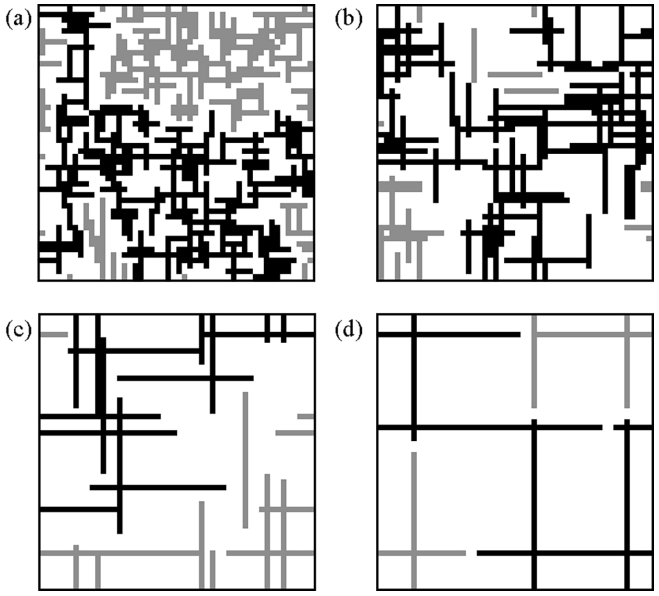

FIG. 2. Snapshots of percolation clusters on the square grid with edge size $L = 50$ formed by slots of different length: (a) $l = 5$; (b) $l = 10$; (c) $l = 25$; (d) $l = 48$. Closed cells: white; the spanning cluster: black; open cells which do not belong to the spanning cluster: grey.

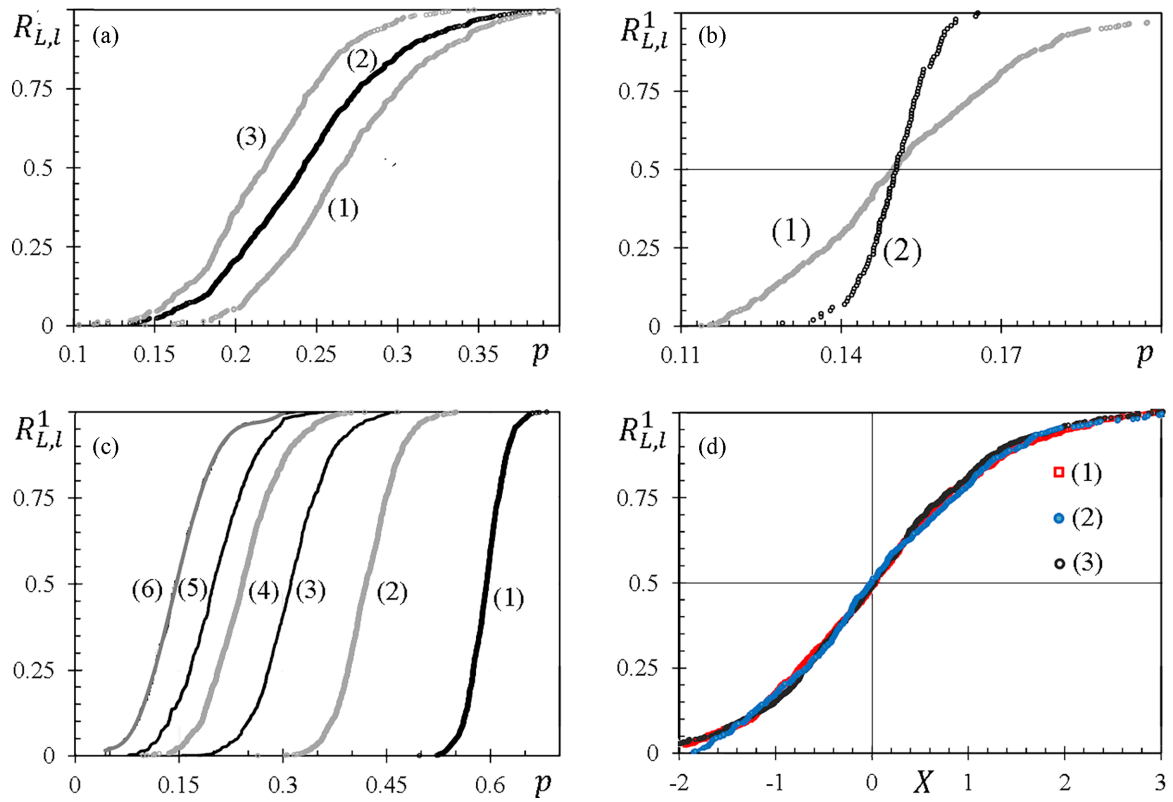

FIG. 3. Typical graphs of (a) spanning probabilities $R^{\rm both}_{L,l}(p)$ (1), $R^{1}_{L,l}(p)$ (2), and $R^{\rm or}_{L,l}(p)$ (3) for $L = 50$ and $l = 15$; (b) spanning probability $R^{1}_{L,l}(p)$ for slots of length $l = 30$ on the square grids with different edge size $L = 200$ (1), $L = 1000$ (2); (c) spanning probability $R^{1}_{L,l}(p)$ for (d) data collapse in the coordinates $R^{1}_{L,l}$ versus $X = [p - p_C(l)]L^{1/\nu}$ for: $L = 50$ and $l = 15$ (1), $L = 200$ and $l = 30$ (2), and $L = 500$ and $l = 250$ (3).

which were established in Ref. [37] for percolation on the square lattice. The relations between different spanning probabilities are illustrated by the graphs in Fig. 3(a). In the limit of $L \to \infty$ all spanning probabilities converge to the same step function. In particular, for the site percolation on the square lattice, it was established that the spanning probability at the percolation threshold $R^{1}_{L}(p_C) \to 1/2$ as $L \to \infty$ [38], while the finite-system estimates of the percolation threshold $p_C(L)$ converge to the bulk value p_C as [39,40]

$$p_{CL} - p_C \propto cL^{-1-1/\nu}, \tag{3}$$

where c is a system-dependent constant and ν is the critical exponent characterizing the divergence of the correlation length $\xi_C \propto |p - p_C|^{-\nu}$.

In this work, we ascertain that the slot percolation on square grids also displays the convergence

$$R^{1}_{L,l}[p_{CL}(l)] \to 1/2 \tag{4}$$

as $L \to \infty$ for any $1 \leqslant l \leqslant L-1$ [see, for example, Fig. 3(b)], while p_C depends on the slot length [see, for instance, Fig. 3(c)]. In this regard, we found that the data of Monte Carlo simulations with different pairs of $(l,\ L)$ can be collapsed on a single curve in the plot

$$R^{1}_{L,l} \text{ versus } X = [p - p_{CL}(l)]L^{1/\nu}, \tag{5}$$

as it is shown in Fig. 3(d). Equations (4) and (5) allow us to estimate the critical concentration of open cells $p_C(l)$ as a function of slot length l. The data collapse in coordinates (5) also allows us to estimate the correlation length exponent ν [41].

Another quantity of interest is the critical exponent β which governs the scaling behavior of percolation strength $P_{L,l} \propto (p - p_{CL})^{\beta}$. The percolation strength is defined as the probability that the open cell belongs to the percolation cluster. Accordingly, the number of open slots in the percolation cluster on the grid of size $L \times L$ scales with the grid size as

$$V_C(p_{C,l}) \propto L^{D}, \tag{6}$$

where $D = 2-\beta/\nu$ is the fractal dimension of the percolation cluster. This allows us to estimate the critical exponent β from the scaling behavior (6) [41]. All other critical exponents can be calculated using the scaling relations between them and the values of ν and β [42].

III. NUMERICAL FINDINGS AND DISCUSSIONS

In Fig. 4(a) the data of numerical simulations are plotted in the coordinates p_C versus l. The critical filling factor $\eta_C(l)$ is related to $p_C(l)$ by Eq. (1), as this is for the continuum percolation. Accordingly, we found that the critical filling factor can be well fitted by the following relationship:

$$\eta_C(l) = -\ln(1 - p_C) = \eta_1/[1 + c(l-1)], \tag{7}$$

as shown in Fig. 4(b), where $\eta_1 = \eta_C(l = 1) = -\ln(1 - 0.592746) = 0.8983\ldots$ and $c = 0.149 \pm 0.001$ is the fitting constant. In this regard, we note that for very large $l \to \infty$

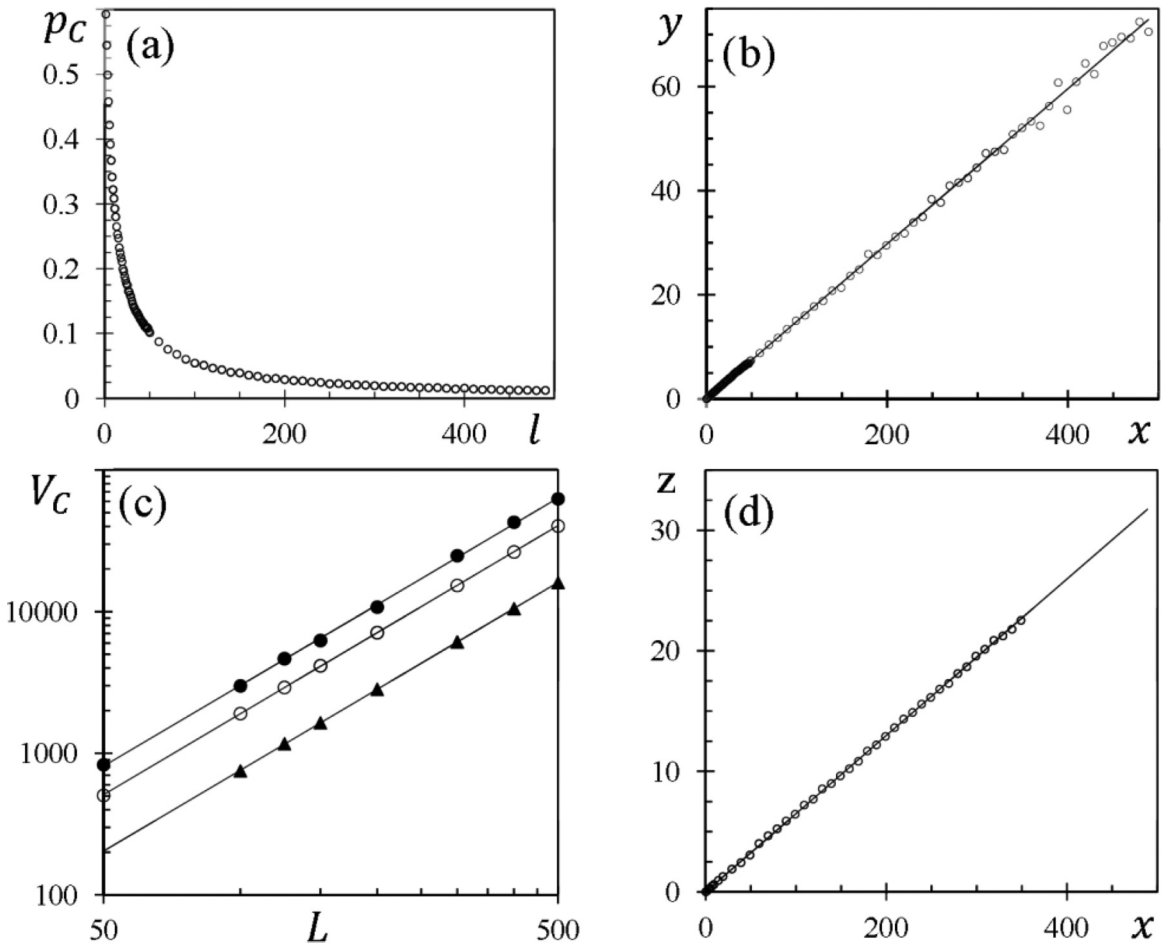

FIG. 4. Graphs of (a) percolation threshold p_C versus slot length l; (b) $y = \eta_C^{-1} - 1$ versus $x = l-1$; circles: data of numerical simulations; straight line: data fitting with Eq. (7); (c) number of open cells in the spanning cluster $V_C(p_C)$ versus grid size L for slots of length $l = 1$ (full circles), 10 (open circles), 500 (triangles); symbols: data of numerical simulations; straight line: data fitting with Eq. (11) (d) $z = (0.5/f) - 1$ versus $x = l-1$; circles: data of simulations; straight line: data fitting with Eq. (12).

the critical filling factor (7) obeys the asymptotic relation

$$\eta_C = \eta_1/(cl) = k/l \tag{8}$$

with $k = \eta_1/c = 6.01 \pm 0.05$. Taking into account that $\eta_C = lwN_C/L^2 = l\mathcal{N}_C$, while $w = 1$ and $\mathcal{N}_C = N_C/L^2$ is the critical number of slots per unit area, Eq. (8) can be rewritten in the form

$$\mathcal{N}_C l^2 = k, \tag{9}$$

which coincides with the relation established in [7,30] for the continuum percolation of widthless sticks. Thus the slot percolation model interpolates between the site percolation on the square lattice ($l = 1$) and the continuous percolation of widthless slits ($l \to \infty$) aligned in two orthogonal directions. Notice that in the last case the expected value of

$$k = \eta_1/c = 6.01 \pm 0.05 \tag{10}$$

is larger than the value of $k = 5.63726 \pm 0.00002$, which was established in [43] for the continuum percolation of randomly oriented widthless sticks.

From the data collapse in the coordinates (5) we found that $\nu = 1.32 \pm 0.01$. This value is consistent with the universal exponent $\nu = 4/3$ expected for the Bernoulli percolation in two dimensions. Furthermore, we found that the number of open cells in the spanning cluster scales with the grid size as

$$V_C(p_C) = f(l)L^D, \tag{11}$$

where $f(l)$ is found to be a function of the slot length [see Fig. 4(c)]. Specifically, we found that the data of numerical simulations can be well fitted using the following approximation:

$$f(l) = a/[1 + b(l-1)] \tag{12}$$

as shown in Fig. 4(d) with the fitting constants equal to $a = 0.50 \pm 0.01$ and $b = 0.064 \pm 0.006$, respectively. So, we found that the fractal dimension of percolation clusters is equal to $D = 1.895 \pm 0.007$. Consequently, we calculate the scaling exponent $\beta = (2-D)\nu = 0.139 \pm 0.008$. Thus the values of both critical exponents (ν and β) are consistent with the universal values ($\nu = 4/3$ and $\beta = 5/36$) expected for the Bernoulli percolation in two dimensions. This indicates that the studied model of slot percolation belongs to the same universality class.

Formation of fracture network in a solid material can be modeled as a percolation of individual cracks. Accordingly, the slot percolation model can be used to study the emergence of fracture networks in porous media. The total porosity of the model medium ϕ is equal to the number of open cells divided on the number of cells in the grid ($L \times L$). The model is essentially discrete and so the critical porosity is $\phi_C(l) = p_C(l)$. The open porosity associated with the connected cracks is equal to $\phi_O = \phi_C P_{L,l}(p_C) = V_C/L^2$. Notice that for larger l the open porosity is much less than the total one.

IV. CONCLUSIONS

In this work we study the percolation of straight slots of square grids with different edge size. The percolation thresholds and critical exponents were found by extensive numerical simulations along with a finite scaling analysis. From the numerical data we acquire the functional dependencies of the critical filling factor and percolation strength on the slot length. This allows us to establish that the slot percolation model interpolates between the site percolation on square lattice ($l = 1$) and the continuous percolation of widthless slicks ($l \to \infty$) aligned in two orthogonal directions. In this way we found that in the case of sticks aligned along two orthogonal directions the critical number of widthless slicks per unit area at the percolation threshold is larger than in the case of randomly oriented sticks. This finding can be verified by direct numerical simulations of the continuum percolation of orthogonally aligned sticks on the plane. We also ascertained that the slot percolation belongs to the same universality class as the standard Bernoulli percolation regardless the length of the percolating slots. Future research with the slot percolation model may explore different distributions of the slot lengths.

ACKNOWLEDGMENT

This research was supported by the National Polytechnic Institute of Mexico under the Project Grants No. 20240771 and No. 20241194.

[1] H. E. Stanley, Application of fractal concepts to polymer statistics and to anomalous transport in randomly porous media, J. Stat. Phys. **36**, 843 (1984).
[2] M. Sahimi, *Applications of Percolation* (Taylor & Francis, London, 1994).
[3] M. Li, R. R. Liu, L. Lü, M. B. Hu, S. Xu, and Y. C. Zhang, Percolation on complex networks: Theory and application, Phys. Rep. **907**, 1 (2021).
[4] R. M. Ziff, Percolation and the pandemic, Phys. A (Amsterdam, Neth.) **568**, 125723 (2021).
[5] J. W. Essam, Percolation theory, Rep. Prog. Phys. **43**, 833 (1980).
[6] V. K. S. Shante and S. Kirkpatrick, An introduction to percolation theory, Adv. Phys. **20**, 325 (1971).
[7] G. E. Pike and C. H. Seager, Percolation and conductivity: A computer study, Phys. Rev. B **10**, 1421 (1974).
[8] G. Kondrat and A. Pekalski, Percolation and jamming in random sequential adsorption of linear segments on a square lattice, Phys. Rev. E **63**, 051108 (2001).
[9] G. Kondrat, Impact of composition of extended objects on percolation on a lattice, Phys. Rev. E **78**, 011101 (2008).
[10] Lj. Budinski-Petkovic, I. Loncarevic, M. Petkovic, Z. M. Jakšic, and S. B. Vrhovac, Percolation in random sequential adsorption of extended objects on a triangular lattice, Phys. Rev. E **85**, 061117 (2012).
[11] G. Kondrat, Z. Koza, and P. Brzeski, Jammed systems of oriented needles always percolate on square lattices, Phys. Rev. E **96**, 022154 (2017).
[12] L. S. Ramirez, P. M. Centres, and J. A. Ramirez-Pastor, Standard and inverse bond percolation of straight rigid rods on square lattices, Phys. Rev. E **97**, 042113 (2018).
[13] Y. Yu. Tarasevich, N. I. Lebovka, and V. V. Laptev, Percolation of linear k-mers on a square lattice: From isotropic through partially ordered to completely aligned states, Phys. Rev. E **86**, 061116 (2012);[]
[14] R. C. Hart and F. D. A. A. Reis, Random sequential adsorption of polydisperse mixtures on lattices, Phys. Rev. E **94**, 022802 (2016).
[15] L. S. Ramírez, P. M. Centres, and J. A. Ramirez-Pastor, Percolation phase transition by removal of k^2-mers from fully occupied lattices, Phys. Rev. E **100**, 032105 (2019).
[16] Z. Koza, G. Kondrat, and K. Suszczyński, Percolation of overlapping squares or cubes on a lattice, J. Stat. Mech. (2014) P11005.
[17] Z. Koza and J. Poła, From discrete to continuous percolation in dimensions 3 to 7, J. Stat. Mech. (2016) 103206.
[18] I. Balberg, C. H. Anderson, S. Alexander, and N. Wagner, Excluded volume and its relation to the onset of percolation, Phys. Rev. B **30**, 3933 (1984).
[19] Z. Neda, R. Florian, and Y. Brechet, Reconsideration of continuum percolation of isotropically oriented sticks in three dimensions, Phys. Rev. E **59**, 3717 (1999).
[20] F. Coupette, A. Härtel, and T. Schilling, Continuum percolation expressed in terms of density distributions, Phys. Rev. E **101**, 062126 (2020).
[21] D. Lara and Vericat F, Percolation behavior of long permeable objects: A reference interaction-site-model study, Phys. Rev. B **40**, 353 (1989).
[22] D. R. Baker, G. Paul, S. Sreenivasan, and H. E. Stanley, Continuum percolation threshold for interpenetrating squares and cubes, Phys. Rev. E **66**, 046136 (2002).
[23] Y. Yu. Tarasevich and A. V. Eserkepov, Percolation thresholds for discorectangles: Numerical estimation for a range of aspect ratios, Phys. Rev. E **101**, 022108 (2020).
[24] F. Coupette, R. de Bruijn, P. Bult, S. Finner, M. A. Miller, P. van der Schoot, and T. Schilling, Nearest-neighbor connectedness theory: A general approach to continuum percolation, Phys. Rev. E **103**, 042115 (2021).
[25] M. Sahimi, Non-linear and non-local transport processes in heterogeneous media: From long-range correlated percolation to fracture and materials breakdown, Phys. Rep. **306**, 213 (1998).
[26] A. Hunt, R. Ewing, and B. Ghanbarian, *Percolation Theory for Flow in Porous Media* (Springer, Berlin, 2014).
[27] A. A. Moreira, C. L. N. Oliveira, A. Hansen, N. A. M. Araújo, H. J. Herrmann, and J. S. Andrade, Fracturing highly disordered materials, Phys. Rev. Lett. **109**, 255701 (2012).

[28] A. Shekhawat, S. Zapperi, and J. P. Sethna, From damage percolation to crack nucleation through finite size criticality, Phys. Rev. Lett. **110**, 185505 (2013).

[29] J. F. Thovert, V. V. Mourzenko, and P. M. Adler, Percolation in three-dimensional fracture networks for arbitrary size and shape distributions, Phys. Rev. E **95**, 042112 (2017).

[30] J. Li and M. Östling, Percolation thresholds of two-dimensional continuum systems of rectangles, Phys. Rev. E **88**, 012101 (2013).

[31] I. Balberg and N. Binenbaum, Computer study of the percolation threshold in a two-dimensional anisotropic system of conducting sticks, Phys. Rev. B **28**, 3799 (1983).

[32] M. Žeželj, I. Stanković, and A. Belić, Finite-size scaling in asymmetric systems of percolating sticks, Phys. Rev. E **85**, 021101 (2012).

[33] Y. Y. Tarasevich and A. V. Eserkepov, Percolation of sticks: Effect of stick alignment and length dispersity, Phys. Rev. E **98**, 062142 (2018).

[34] T. Manzocchi, The connectivity of two-dimensional networks of spatially correlated fractures, Water Resour. Res. **38**, 1162 (2002).

[35] D. Healy, R. E. Rizzo, D. G. Cornwell, N. J. C. Farrell, H. Watkins Farrell, N. E. Timms, E. Gomez-Rivas, and M. Smith, FracPaQ: A MATLAB^{TM} toolbox for the quantification of fracture patterns, J. Struct. Geol. **95**, 1 (2017).

[36] H. Mondragón-Nava, D. Samayoa, B. Mena, and A. S. Balankin, Fractal features of fracture networks and key attributes of their models, Fractal Fract. **7**, 509 (2023).

[37] F. Yonezawa, S. Sakamoto, and M. Hori, Percolation in two-dimensional lattices. I. A technique for the estimation of thresholds, Phys. Rev. B **40**, 636 (1989).

[38] J. Bernasconi, Real-space renormalization of bond-disordered conductance lattices, Phys. Rev. B **18**, 2185 (1978).

[39] R. M. Ziff, Spanning probability in 2D percolation, Phys. Rev. Lett. **69**, 2670 (1992).

[40] R. M. Ziff and M. E. J. Newman, Convergence of threshold estimates for two-dimensional percolation, Phys. Rev. E **66**, 016129 (2002).

[41] A. S. Balankin, M. A. Martínez-Cruz, O. Susarrey-Huerta, and L. Damian-Adame, Percolation on infinitely ramified fractal networks, Phys. Lett. A **382**, 12 (2018).

[42] D. Stauffer, Scaling theory of percolation clusters, Phys. Rep. **54**, 1 (1979).

[43] J. Li and S. L. Zhang, Finite-size scaling in stick percolation, Phys. Rev. E **80**, 040104(R) (2009).